Oxidative Strong Metal–Support Interactions

Subjects: Chemistry, Applied

Contributor: Botao Qiao

Oxidative Strong Metal–Support Interactions (OMSI) can be defined as a phenomenon occurring in a supported metal catalyst that is triggered by oxidative (or non-reductive) conditions with the typical features resembling that of SMSI, including 1) small-molecule of CO or H2 adsorption on metal will be significantly suppressed, 2) the support would encapsulate metal particles, 3) electron transfer from metal to the support, and 4) a reversal of the above phenomena following reduction treatment.

Keywords: oxidative strong metal–support interactions ; strong metal–support interaction ; supported metal catalyst ; metal-oxide interfaces ; charge transfer ; heterogeneous catalysis

1. Introduction

Strong metal-support interaction (SMSI) is a phenomenon discovered by Tauster et al in the late 1970s, that TiO_2 supported Pt-group metals will lose their capability to adsorb small molecules (such as CO and H_2) following high-temperature reduction. [1][2] SMSI between Pt-group metals and reducible oxides has continuously been studied in both catalysis application and surface science for the next three decades, and the understanding on it has progressed significantly. The classical SMSI theory thus developed, based on which the SMSI-active catalyst system was limited. Au (and IB group metals), with a relatively lower work function and surface energy respect to Pt-group metals, had thus been regarded as SMSI-inert for a long time. [3][4][5][6]

A breakthrough came from Mou's group in 2012.[7] They found an oxygen-induced SMSI phenomenon in an Au/ZnO-nanorod catalyst, that, following oxidation under 300 °C, the Au nanoparticles will be encapsulated by ZnO accompanied by electron transfer from Au to the support, which will be reversed by hydrogen treatment. This work, for the first time, not only extended the conditions for evoking SMSI but also opened a prelude for the study of SMSI in Au-based catalysts. Only about four years later, a similar oxidative SMSI phenomenon was revealed by Tang et al. in nonoxide (hydroxyapatite and phosphate)-supported Au catalysts, expanding the territory of SMSI to the non-oxide support system.[8] Furthermore, in 2018, they confirmed that the nonoxide- and ZnO-supported Pt-group metals are also applicable for this oxygen-induced SMSI, and formally proposed the concept of "oxidative strong metal–support interactions (OMSI)" to distinguish from classical SMSI, which was triggered by reductive conditions.[9] It has been proved that controlled OMSI is effective in tuning the catalyst performances,[7][8][9][10] and a few discoveries inspired by OMSI were consecutively reported thereafter, such as uncovering the classical SMSI between Au (actually the IB group metals) and TiO_2, and SMSI between Au and layered double hydroxide support.[11][12]

OMSI has not only shed new light on the understanding of SMSI phenomena but also provided new opportunities for the design and development of high-performance catalysts, thus becoming an important part of the generalized SMSI field.

2. Features, and Catalyst Systems of OMSI

OMSI can be defined as a phenomenon occurring in supported metal catalyst that triggered by oxidative (or non-reductive) conditions with the typical features resemble with that of SMSI. Current OMSI systems involve ZnO-nanorod supported Au, nonoxides (hydroxyapatite and phosphate) supported Au and Pt-group metals, and ZnO supported Pt-group metals (Figure 1). The common characteristics of OMSI evoked by high-temperature oxidation (or an inert atmosphere) can be summarized as: (1) small-molecule of CO or H_2 adsorption on metal will be significantly suppressed; (2) mass transport that the support would encapsulate metal particles; (3) electron transfer from metal to the support resulting in a positively charged metal species; and (4) a reversal of the above phenomena following reduction treatment. The comparison of the inducing conditions and main characteristics of OMSI and the classical SMSI was listed in **Table 1**.

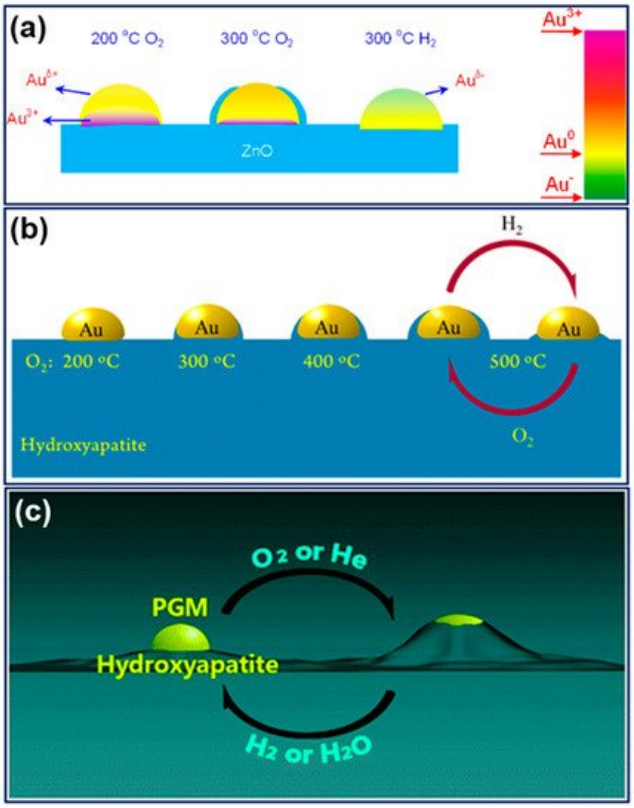

Figure 1. Schematic illustration of OMSI in (**a**) Au/ZnO-nanorod, reproduced with permission from [7], Copyright 2012 American Chemical Society, (**b**) Au/HAP, reproduced with permission from [8], Copyright 2016 American Chemical Society, and (**c**) HAP supported Pt-group metals, reproduced with permission from [9], Copyright 2018 The Royal Society of Chemistry.

Table 1. Comparison between OMSI and classical SMSI.

	Classical SMSI	OMSI
typical catalyst system	**reducible oxide-supported Au or Pt-group metals**	**HAP- or ZnO-supported Au or Pt-group metals**
inducing conditions	**high-temperature reduction**	**high-temperature oxidation**
suppression of adsorption	**yes**	**yes**
mass transport (encapsulation)	**yes**	**yes**
electron transfer	**support to metal**	**metal to support**
reversibility	**yes**	**yes**

3. Identification and Characterization of OMSI

The abovementioned four typical features are also the criteria for the identification of OMSI occurrence, which generally needs a combination of multiple characterization methods to confirm.

3.1. Adsorption Behavior

One of the most typical spectroscopic techniques is the in situ molecular probe infrared (IR) spectroscopy. Due to site-specific sensitivity in detecting the adsorption property of metal surface, it has been popularized in heterogeneous catalysis and become an indispensable approach to measure adsorption behavior of catalysts in the SMSI study.[13][7][8][9][10][11][12][14]

Tang et al. carried out an in situ diffuse reflectance infrared Fourier transform spectroscopy (DRIFTS) measurement of CO adsorption on Au/HAP treated by high-temperature oxidation under different temperatures, an instructive case for the application of IR spectroscopy to the identification of OMSI.[8] As shown in **Figure 2**a, the bands at 2102~2110 cm^{-1} were ascribed to the CO adsorbed on the Au surface (CO-Au). Similar measurements were further carried out to prove the reversible suppression of chemisorption on Pd/HAP and Pt/HAP by high-temperature oxidation/reduction, confirming the occurrence of OMSI in Pt-group metal-based catalysts (**Figure 2**b,c).[9]

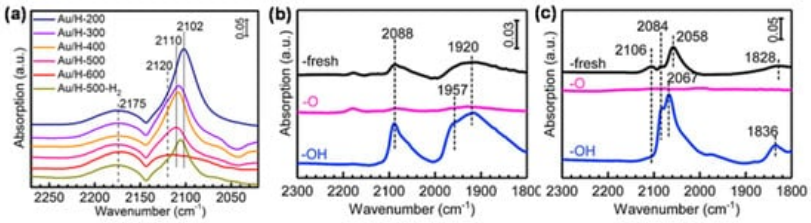

Figure 2. (**a**) In situ DRIFT spectra of CO adsorption on Au/H-X (H: HAP; X: the calcination temperature) and Au/H-500-H_2 (obtained by further reducing Au/H-500 at 500 °C); the bands at 2175 and 2120 cm^{-1} can be assigned to the gas CO. Reproduced with permission from [8], copyright: 2016 by the American Chemical Society. (**b**,**c**) In situ DRIFT spectra of CO adsorption on (**b**) Pd/HAP and (**c**) Pt/HAP samples. "-fresh" represents the freshly synthesized samples without calcination, "-O" represents samples calcined under 10 vol% O_2/He flow at 500 °C, "-OH" represents samples further reduced under 10 vol% H_2/He flow at 250 or 500 °C for Pd/HAP and Pt/HAP, respectively. Reproduced with permission from [9], copyright: 2018 by The Royal Society of Chemistry.

3.2. Mass Transport

Mass transport in OMSI mainly refers to the reversible encapsulation of metal by the deformed support, which generally can be intuitively observed by high resolution transmission electron microscopy (HRTEM). In 1985, Singh et al. directly observed a thin overlayer on the Rh surface through HRTEM in Rh/TiO_2 where SMSI occurred, thus inferring that the overlayer inhibited the adsorption of small molecules on the catalyst.[15] Since then, the SMSI-provoked encapsulation phenomenon has been found in various catalysts, becoming an essential basis for identifying the occurrence of SMSI, and HRTEM thus became indispensable.

By HRTEM, Tang et al. found that the coverage of HAP on Au nanoparticles depended on the calcination temperature.[8] As shown in **Figure 3**a–e, the encapsulation layer on the surface of Au nanoparticle appeared when the Au/HAP calcined at 300 °C, then the layer gradually spread as the calcination temperature increased, and finally completely wrapped the Au nanoparticle after being calcined at 600 °C. By subsequent treatment under pure H_2 at 500 °C, the encapsulation layer retreated (**Figure 3**f).

Verifying the composition of the encapsulation layer is critical to concrete the mass transport of the support. For most SMSI or OMSI systems, the encapsulation layer is generally amorphous, which could not be determined by measuring the lattice spacing. The electron energy loss spectrum (EELS) is powerful to analyze the composition and the element valence of materials, thus has long been used in SMSI studies.[16][17][18] For instance, the cover layer on Au nanoparticles in the Au/HAP calcined at 600 ^oC was detected by EELS and the result (**Figure 3g**) showed the layer was composed of P, Ca and O, confirming it was derived from the HAP support.[8]

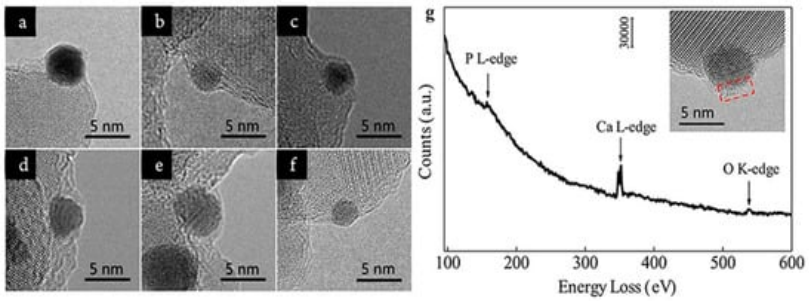

Figure 3. (**a**–**e**) HRTEM images of Au/H-X samples where "H" represents HAP and "X" represents the calcination temperature: (**a**) Au/H-200, (**b**) Au/H-300, (**c**) Au/H-400, (**d**) Au/H-500, and (**e**) Au/H-600; (**f**) HRTEM image of sample obtained by further reducing Au/H-500 at 500 °C under H_2. (**g**) The electron energy loss spectrum (EELS) spectrum of Au/H-600 where the Au nanoparticles were completely encapsulated. Reproduced with permission from [8], copyright: 2016 by the American Chemical Society.

3.3. Electron Transfer

Generally, the electron transfer during OMSI is mainly manifested by the perturbation in the valence state and the change in electronic structure of the supported metal, which can be examined by element-specific spectroscopic techniques that are sensitive to chemical state and atomic structure. Earlier for the research of classical SMSI, X-ray photoelectron spectroscopy (XPS), ultraviolet photoelectron spectroscopy (UPS), and Auger electron spectroscopy (AES) have been employed in characterizing the high-temperature reduction-induced chemical state changes of metal.[19][20][21][16][17][22][23] The aforementioned CO-probed IR spectroscopy can also be used to testify the phenomenon of electron transfer as it is

sensitive to the metal electronic structure. On the other hand, the electron transfer that accompanied by the support deformation at interface will inevitably impact the surface local coordination structure of the support. For the oxide support-based catalysts, the SMSI- or OMSI-induced electron perturbation can be verified by electron paramagnetic resonance (EPR), a technique sensitive to species with unpaired electrons such as oxygen vacancies or metal ions in paramagnetic valence states.[24][25][26][27] The metal atom-centered local coordination structure that strongly depends on the interaction between metal and the support can be examined by X-ray absorption spectroscopy (XAS), which is also necessary in SMSI and OMSI studies.[22][28][29]

4. Application and Influence of OMSI

The SMSI effect is able to alter the catalyst properties of the adsorption capacity, interface structure, and the electronic state, thus it has been extensively applied to enhance the catalyst performance for diverse reactions and recognized to be a highly effective method currently.[14][30][31][32][33][34][35][36][37][38][39][40] Admittedly, realizing the appropriate state of SMSI for different reactions is critical and difficult, which is limited by the precondition for the initiation and maintenance of SMSI. For instance, high-temperature reduction or a reductive atmosphere is prerequisite for classical SMSI, therefore the application of classical SMSI in non-reducing conditions is constrained. On this premise, discovery of the OMSI effect will enrich the potential application of the metal–support interaction under specific conditions to a large extent. On the other hand, OMSI truly broadens the territory of metal–support interaction, inspiring more explorations on similar phenomena that occurred in catalysts with multiple metals and supports and evoked by various conditions. This is of great value in in-depth cognition of metal–support interaction and catalytic mechanism.

4.1. Enhancing Catalyst Performance by Tuning the OMSI

When OMSI was evoked and the encapsulation layer formed, metal nanoparticles were restrained on the support, thus they will be prevented from aggregation or leaching during reaction. Tang et al. compared the recycle performance of Au/HAP catalysts calcined at 200 and 500 °C for the selective oxidation of benzyl alcohol.[8] As shown in **Figure 4**a,b, both conversion and selectivity of the catalyst calcined at 500 °C (Au/H-500) remained unchanged after five cycles of use, and no Au loss was detected. However, the Au/HAP that calcined at 200 ^{o}C (Au/H-200) without encapsulation layer formed has seriously deactivated in the first three reaction cycles, and the used catalyst showed sintered Au nanoparticles and decreased loading. Similarly, reusability of Pd/HAP for Suzuki cross-coupling was significantly enhanced by calcining at 500 ^{o}C (**Figure 4c**).[9] Moreover, as shown in **Figure 4d**, Pt/HAP calcined at 500 ^{o}C (Pt/HAP-O) exhibited excellent durability under a simulated auto-emission control reaction condition, that the CO oxidation conversion kept unchanged during a 40 hour test under 400 ^{o}C, which is distinctly better than the Pt/TiO_2 reduced at 500 ^{o}C (Pt/TiO_2-H500, where classical SMSI formed) that deactivated severely in the first 5 hours.[9] These evidently demonstrated the formation of OMSI can effectively inhibit the leaching and aggregation of metal species during reactions in liquid-phase or under elevated temperature with oxidative atmosphere, which is of great importance for practical application.

Catalyst activity mostly depends on the interface sites, which would be impacted by encapsulation when SMSI was evoked. Meanwhile, limited by the support type, catalysts that are able to form SMSI may not be particularly active for certain reactions, although the stability can be enhanced. Controlled SMSI state therefore is needed to obtain catalysts with both improved stability and activity. Commendably, Tang et al. developed an ultrastable Au nanocatalyst with high activity by tuning the OMSI between Au and the composite support TiO_2-HAP.[10] As shown in **Figure 5**, the Au nanoparticle was located at the interfacial regions between the TiO_2 and HAP.

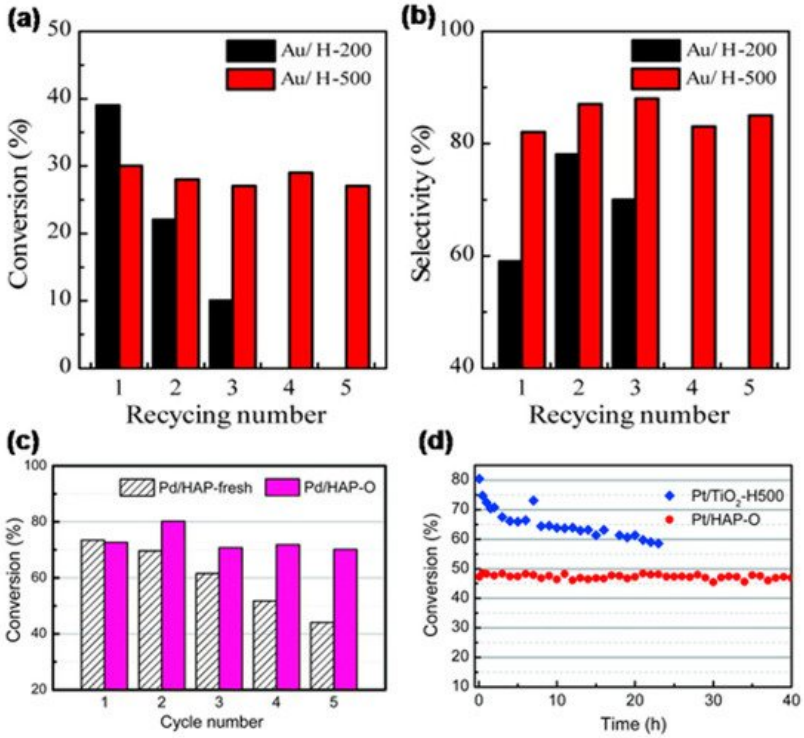

Figure 4. (**a**) Conversion and (**b**) selectivity of benzyl alcohol over Au/H-200 and Au/H-500. Reproduced with permission from [8], copyright: 2016 by the American Chemical Society. (**c**) Cycling performance of Pd/HAP-fresh and Pd/HAP-O for the Suzuki cross-coupling reaction. (**d**) CO conversion versus reaction time of Pt/HAP-O and Pt/TiO_2-H500 samples at 400 °C. Space velocity of Pt/HAP-O and Pt/TiO_2-H500 were ~1,690,000 and 1,100,000 L g_{Pt}^{-1} h^{-1}, respectively. Reproduced with permission from [9], copyright: 2018 by The Royal Society of Chemistry.

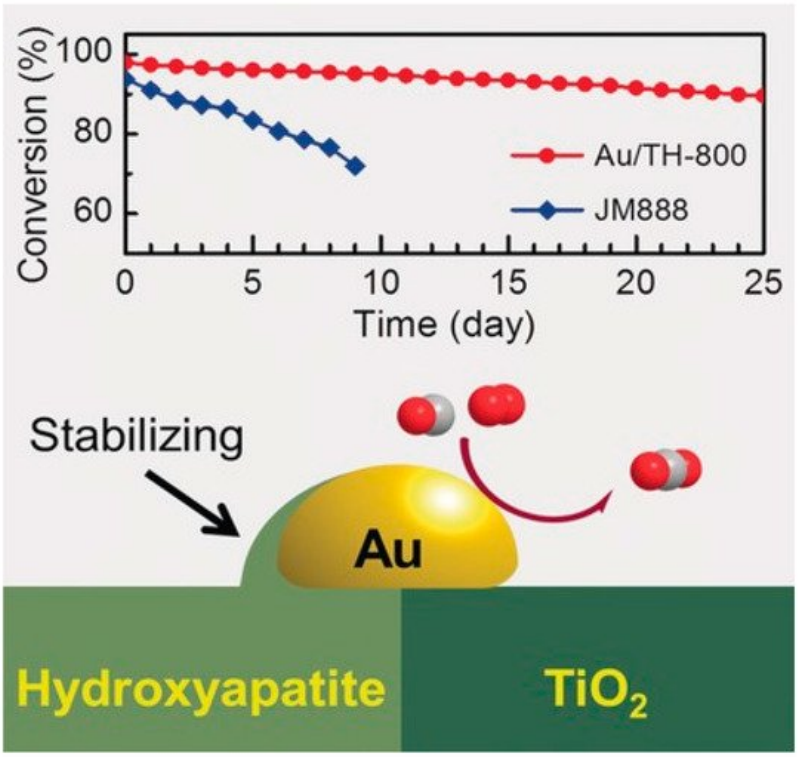

Figure 5. Schematic illustration of TiO_2-HAP supported Au nanocatalyst with high stability owing to the OMSI between Au and HAP with TiO_2, where the upper part shows CO conversion versus reaction time of the Au/TH-800 and commercial three way catalyst JM888 at 400 °C. Reproduced with permission from [10], copyright: 2016 John Wiley and Sons.

4.2. Discoveries Inspired by or Based on OMSI

Tang et al. synthesized TiO_2-supported Au nanocatalysts and further investigated their adsorption performance, mass transport, and electronic state changes under high-temperature reduction, unequivocally uncovering a classical SMSI in Au/TiO_2 (**Figure 6**), and further extended to other reducible oxide (such as CeO_2 and Fe_3O_4)-supported Au and TiO_2-supported IB group metal (Ag and Cu) catalysts.[11] This work is a pivotal breakthrough in promoting SMSI research that

verified the universality of the classical SMSI phenomenon and complemented the catalyst system of metal–support interactions (**Figure 7**). Based on this work, more recently, the size-dependency of classical SMSI was further revealed in Au/TiO_2 nanocatalysts, where larger Au particles are more prone to be encapsulated than smaller ones, which brings an in-depth understanding of the SMSI phenomenon and provides a new approach to refine catalyst performance.[14]

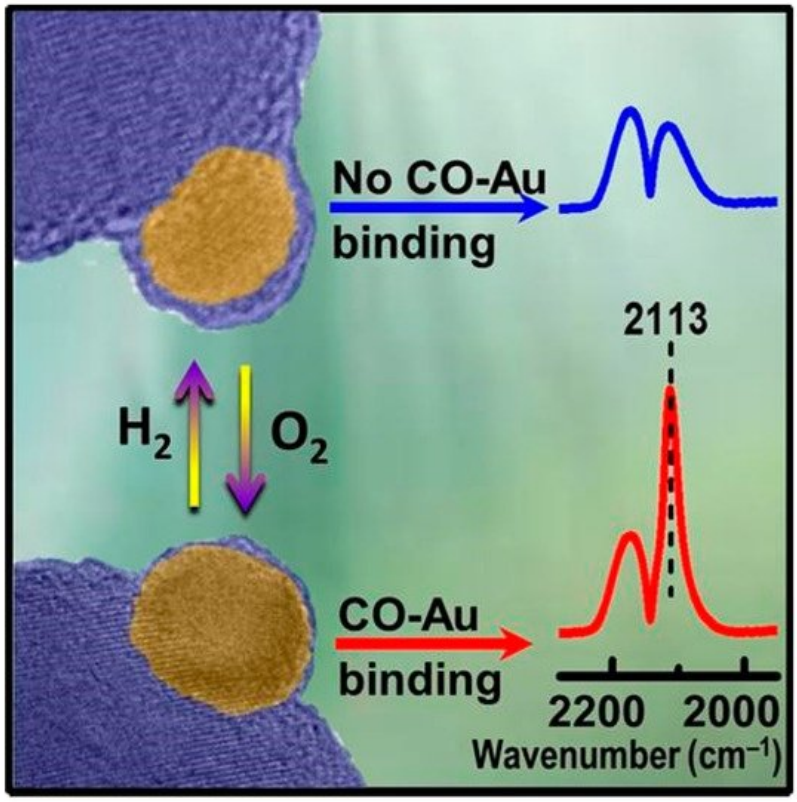

Figure 6. Schematic illustration of the classical SMSI phenomenon in Au/TiO_2. Reproduced with permission from [11], copyright: 2017 by the American Association for the Advancement of Science.

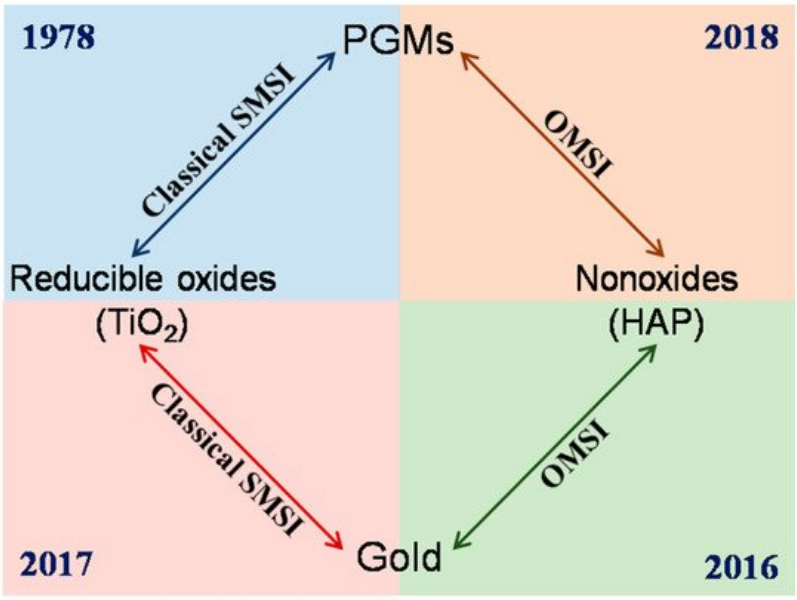

Figure 7. Schematic illustration of the catalyst systems for classical SMSI and OMSI.

References

1. S. J. Tauster; S. C. Fung; R. L. Garten; Strong metal-support interactions. Group 8 noble metals supported on titanium dioxide. *Journal of the American Chemical Society* **1978**, *100*, 170-175, 10.1021/ja00469a029.
2. S Tauster; S. C. Fung; Strong metal-support interactions: Occurrence among the binary oxides of groups IIA?VB. *Journ al of Catalysis* **1978**, *55*, 29-35, 10.1016/0021-9517(78)90182-3.

3. François Pesty; Hans-Peter Steinrück; Theodore E. Madey; Thermal stability of Pt films on TiO2(110): evidence for enc apsulation. *Surface Science* **1995**, *339*, 83-95, 10.1016/0039-6028(95)00605-2.

4. Y. Gao; Y. Liang; S.A. Chambers; Thermal stability and the role of oxygen vacancy defects in strong metal support inter action — Pt on Nb-doped TiO2(100). *Surface Science* **1996**, *365*, 638-648, 10.1016/0039-6028(96)00763-7.

5. Lei Zhang; Rajendra Persaud; Theodore E. Madey; Ultrathin metal films on a metal oxide surface: Growth of Au onTiO2 (110). *Physical Review B* **1997**, *56*, 10549-10557, 10.1103/physrevb.56.10549.

6. D. W. Goodman; ?Catalytically active Au on Titania:? yet another example of a strong metal support interaction (SMS I)?. *Catalysis Letters* **2005**, *99*, 1-4, 10.1007/s10562-004-0768-2.

7. Xiaoyan Liu; Ming-Han Liu; Yi-Chia Luo; Chung-Yuan Mou; Shawn D. Lin; Hongkui Cheng; Jin-Ming Chen; Jyh-Fu Lee; Tien-Sung Lin; Strong Metal–Support Interactions between Gold Nanoparticles and ZnO Nanorods in CO Oxidation. *Jo urnal of the American Chemical Society* **2012**, *134*, 10251-10258, 10.1021/ja3033235.

8. Hailian Tang; Jiake Wei; Fei Liu; Botao Qiao; Xiaoli Pan; Lin Li; Jingyue (Jimmy) Liu; Junhu Wang; Tao Zhang; Strong Metal–Support Interactions between Gold Nanoparticles and Nonoxides. *Journal of the American Chemical Society* **20 15**, *138*, 56-59, 10.1021/jacs.5b11306.

9. Hailian Tang; Yang Su; Yalin Guo; Leilei Zhang; Tianbo Li; Ketao Zang; Fei Liu; Lin Li; Jun Luo; Botao Qiao; et al. Oxid ative strong metal–support interactions (OMSI) of supported platinum-group metal catalysts. *Chemical Science* **2018**, *9*, 6679-6684, 10.1039/c8sc01392f.

10. Hailian Tang; Fei Liu; Jiake Wei; Botao Qiao; Kunfeng Zhao; Yang Su; Changzi Jin; Lin Li; Jingyue (Jimmy) Liu; Junhu Wang; et al. Ultrastable Hydroxyapatite/Titanium-Dioxide-Supported Gold Nanocatalyst with Strong Metal–Support Inte raction for Carbon Monoxide Oxidation. *Angewandte Chemie International Edition* **2016**, *55*, 10606-10611, 10.1002/ani e.201601823.

11. Hailian Tang; Yang Su; Bingsen Zhang; Adam F. Lee; Mark A. Isaacs; Karen Wilson; Tang Hailian; Wilson Karen; Jiahui Huang; Masatake Haruta; et al. Classical strong metal–support interactions between gold nanoparticles and titanium di oxide. *Science Advances* **2017**, *3*, e1700231-e1700231, 10.1126/sciadv.1700231.

12. Liang Wang; Jian Zhang; Yihan Zhu; Shaodan Xu; Chengtao Wang; Chaoqun Bian; Xiangju Meng; Feng-Shou Xiao; St rong Metal–Support Interactions Achieved by Hydroxide-to-Oxide Support Transformation for Preparation of Sinter-Resi stant Gold Nanoparticle Catalysts. *ACS Catalysis* **2017**, *7*, 7461-7465, 10.1021/acscatal.7b01947.

13. Gary L. Haller; Daniel E. Resasco; Metal–Support Interaction: Group VIII Metals and Reducible Oxides. *Advances in C atalysis* **1989**, *36*, 173-235, 10.1016/s0360-0564(08)60018-8.

14. Xiaorui Du; Yike Huang; Xiaoli Pan; Bing Han; Yang Su; Qike Jiang; Mingrun Li; Hailian Tang; Gao Li; Botao Qiao; et al. Size-dependent strong metal-support interaction in TiO2 supported Au nanocatalysts. *Nature Communications* **2020**, *1 1*, 5811, 10.1038/s41467-020-19484-4.

15. A Singh; Electron microscopy study of the interactions of rhodium with titania. *Journal of Catalysis* **1985**, *94*, 422-435, 1 0.1016/0021-9517(85)90207-6.

16. Yip-Wah Chung; W. B. Weissbard; Surface spectroscopy studies of the SrTiO3(100) surface and the platinum-SrTiO3(1 00) interface. *Physical Review B* **1979**, *20*, 3456-3461, 10.1103/physrevb.20.3456.

17. S Takatani; Strong metal-support interaction in Ni/Ti02: Auger and vibrational spectroscopy evidence for the segregatio n of TiOx (x $ap;-1) on Ni and its effects on CO chemisorption. *Journal of Catalysis* **1984**, *90*, 75-83, 10.1016/0021-951 7(84)90086-1.

18. Felipe Polo-Garzon; Thomas F. Blum; Zhenghong Bao; Kristen Wang; Victor Fung; Zhennan Huang; Elizabeth E. Bicke l; De-En Jiang; Miaofang Chi; Zili Wu; et al. In Situ Strong Metal–Support Interaction (SMSI) Affects Catalytic Alcohol C onversion. *ACS Catalysis* **2021**, *11*, 1938-1945, 10.1021/acscatal.0c05324.

19. Yip-Wah Chung; Guoxing Xiong; Chia-Chieh Kao; Mechanism of strong metal-support interaction in Ni/TiO2. *Journal of Catalysis* **1984**, *85*, 237-243, 10.1016/0021-9517(84)90126-x.

20. Hassan Sadeghi; SMSI in Rh/TiO2 model catalysts: Evidence for oxide migration*1. *Journal of Catalysis* **1984**, *87*, 279-282, 10.1016/0021-9517(84)90188-x.

21. S. J. Tauster; Strong metal-support interactions. *Accounts of Chemical Research* **1987**, *20*, 389-394, 10.1021/ar00143a 001.

22. Bruce C. Beard; Philip N. Ross; Platinum-titanium alloy formation from high-temperature reduction of a titania-impregna ted platinum catalyst: implications for strong metal-support interaction. *The Journal of Physical Chemistry* **1986**, *90*, 68 11-6817, 10.1021/j100284a020.

23. S. Roberts; R.J. Gorte; A study of the migration and stability of titania on a model Rh catalyst*1. *Journal of Catalysis* **1990**, *124*, 553-556, 10.1016/0021-9517(90)90202-u.

24. J. Sanz; J. M. Rojo; P. Malet; G. Munuera; M. T. Blasco; J. C. Conesa; J. Soria; Influence of the hydrogen uptake by the support on metal-support interactions in catalysts. Comparison of the rhodium/titanium dioxide and rhodium/strontium titanate (SrTiO3) systems. *The Journal of Physical Chemistry* **1985**, *89*, 5427-5433, 10.1021/j100271a023.

25. Catherine Louis; Christine Lepetit; Michel Che; EPR characterization of oxide supported transition metal ions: Relevance to catalysis. *Molecular Engineering* **1994**, *4*, 3-38, 10.1007/bf01004048.

26. Krystyna Dyrek; Michel Che; EPR as a Tool To Investigate the Transition Metal Chemistry on Oxide Surfaces. *Chemical Reviews* **1997**, *97*, 305-332, 10.1021/cr950259d.

27. Ning Liu; Ming Xu; Yusen Yang; Shaomin Zhang; Jian Zhang; Wenlong Wang; Lirong Zheng; Song Hong; Min Wei; Auδ−–Ov–Ti3+ Interfacial Site: Catalytic Active Center toward Low-Temperature Water Gas Shift Reaction. *ACS Catalysis* **2019**, *9*, 2707-2717, 10.1021/acscatal.8b04913.

28. D.R. Short; A.N. Mansour; J.W. Cook Jr.; D.E. Sayers; J.R. Katzer; X-Ray absorption edge and extended x-ray absorption fine structure studies of Pt/TiO2 catalysts. *Journal of Catalysis* **1983**, *82*, 299-312, 10.1016/0021-9517(83)90196-3.

29. Chengwu Qiu; Yaroslav Odarchenko; Qingwei Meng; Peixi Cong; Martin A. W. Schoen; Armin Kleibert; Thomas Forrest; Andrew M. Beale; Direct observation of the evolving metal–support interaction of individual cobalt nanoparticles at the titania and silica interface. *Chemical Science* **2020**, *11*, 13060-13070, 10.1039/d0sc03113e.

30. Yaru Zhang; Xiaoli Yang; Xiaofeng Yang; Hongmin Duan; Haifeng Qi; Yang Su; Binglian Liang; Huabing Tao; Bin Liu; De Chen; et al. Tuning reactivity of Fischer–Tropsch synthesis by regulating TiOx overlayer over Ru/TiO2 nanocatalysts. *Nature Communications* **2020**, *11*, 3185, 10.1038/s41467-020-17044-4.

31. Siwei Li; Yao Xu; Yifu Chen; Weizhen Li; Lili Lin; Mengzhu Li; Yuchen Deng; Xiaoping Wang; Binghui Ge; Ce Yang; et al. Tuning the Selectivity of Catalytic Carbon Dioxide Hydrogenation over Iridium/Cerium Oxide Catalysts with a Strong Metal-Support Interaction. *Angewandte Chemie International Edition* **2017**, *56*, 10761-10765, 10.1002/anie.201705002.

32. Jian Li; Yaping Lin; Xiulian Pan; Dengyun Miao; Ding Ding; Yi Cui; Jinhu Dong; Xinhe Bao; Enhanced CO2 Methanation Activity of Ni/Anatase Catalyst by Tuning Strong Metal–Support Interactions. *ACS Catalysis* **2019**, *9*, 6342-6348, 10.1021/acscatal.9b00401.

33. Carlos Hernández Mejía; Tom W. Van Deelen; Krijn P. De Jong; Activity enhancement of cobalt catalysts by tuning metal-support interactions. *Nature Communications* **2018**, *9*, 4459, 10.1038/s41467-018-06903-w.

34. Avelino Corma; Pedro Serna; Patricia Concepción; José Juan Calvino; Transforming Nonselective into Chemoselective Metal Catalysts for the Hydrogenation of Substituted Nitroaromatics. *Journal of the American Chemical Society* **2008**, *130*, 8748-8753, 10.1021/ja800959g.

35. Min-Sung Kim; Sang-Ho Chung; Chun-Jae Yoo; Myung Suk Lee; Il-Hyoung Cho; Dae-Won Lee; Kwan-Young Lee; Catalytic reduction of nitrate in water over Pd–Cu/TiO2 catalyst: Effect of the strong metal-support interaction (SMSI) on the catalytic activity. *Applied Catalysis B: Environmental* **2013**, *142-143*, 354-361, 10.1016/j.apcatb.2013.05.033.

36. Kazumasa Murata; Daichi Kosuge; Junya Ohyama; Yuji Mahara; Yuta Yamamoto; Shigeo Arai; Atsushi Satsuma; Exploiting Metal–Support Interactions to Tune the Redox Properties of Supported Pd Catalysts for Methane Combustion. *ACS Catalysis* **2019**, *10*, 1381-1387, 10.1021/acscatal.9b04524.

37. Yaru Zhang; Xiong Su; Lin Li; Haifeng Qi; Chongya Yang; Wei Liu; Xiaoli Pan; Xiaoyan Liu; Xiaofeng Yang; Yanqiang Huang; et al. Ru/TiO2 Catalysts with Size-Dependent Metal/Support Interaction for Tunable Reactivity in Fischer–Tropsch Synthesis. *ACS Catalysis* **2020**, *10*, 12967-12975, 10.1021/acscatal.0c02780.

38. Yaru Zhang; Zhen Zhang; Xiaofeng Yang; Ruifeng Wang; Hongmin Duan; Zheng Shen; Lin Li; Yang Su; Runze Yang; Yongping Zhang; et al. Tuning selectivity of CO2 hydrogenation by modulating the strong metal–support interaction over Ir/TiO2 catalysts. *Green Chemistry* **2020**, *22*, 6855-6861, 10.1039/d0gc02302g.

39. Hai Wang; Liang Wang; Dong Lin; Xiang Feng; Yiming Niu; Bingsen Zhang; Feng-Shou Xiao; Strong metal–support interactions on gold nanoparticle catalysts achieved through Le Chatelier’s principle. *Nature Catalysis* **2021**, *4*, 418-424, 10.1038/s41929-021-00611-3.

40. Bingyu Lin; Biyun Fang; Yuyuan Wu; Chunyan Li; Jun Ni; Xiuyun Wang; Jianxin Lin; Chak-Tong Au; Lilong Jiang; Enhanced Ammonia Synthesis Activity of Ceria-Supported Ruthenium Catalysts Induced by CO Activation. *ACS Catalysis* **2021**, *11*, 1331-1339, 10.1021/acscatal.0c05074.

41. Hai Wang; Liang Wang; Dong Lin; Xiang Feng; Yiming Niu; Bingsen Zhang; Feng-Shou Xiao; Strong metal–support interactions on gold nanoparticle catalysts achieved through Le Chatelier’s principle. *Nature Catalysis* **2021**, *4*, 418-424, 10.1038/s41929-021-00611-3.

42. Bingyu Lin; Biyun Fang; Yuyuan Wu; Chunyan Li; Jun Ni; Xiuyun Wang; Jianxin Lin; Chak-Tong Au; Lilong Jiang; Enhanced Ammonia Synthesis Activity of Ceria-Supported Ruthenium Catalysts Induced by CO Activation. *ACS Catalysis* **2021**, *11*, 1331-1339, 10.1021/acscatal.0c05074.